



# Experimental Verification of Prediction Method for Electromigration Failure of Polycrystalline Lines

著者	坂 真澄
journal or publication title	Journal of applied physics
volume	87
number	6
page range	2785-2791
year	2000
URL	<a href="http://hdl.handle.net/10097/35467">http://hdl.handle.net/10097/35467</a>

doi: 10.1063/1.372257

# Experimental verification of prediction method for electromigration failure of polycrystalline lines

Kazuhiko Sasagawa<sup>a)</sup>

*Department of Intelligent Machines and System Engineering, Hirosaki University, 3 Bunkyo-cho, Hirosaki 036-8561, Japan*

Kazushi Naito, Hiroki Kimura, and Masumi Saka

*Department of Mechanical Engineering, Tohoku University, 01 Aoba, Aramaki, Aoba-ku, Sendai 980-8579, Japan*

Hiroyuki Abé

*Tohoku University, 2-1-1 Katahira, Aoba-ku, Sendai 980-8577, Japan*

(Received 26 April 1999; accepted for publication 9 December 1999)

A prediction method for electromigration failure in polycrystalline lines has been proposed using the governing parameter of electromigration damage, the atomic flux divergence ( $AFD_{gen}$ ), and the usefulness has been verified by experiment where various line shapes were treated under various operating conditions. In the prediction method, lifetime and failure site in a metal line have been predicted by numerical simulation of the processes of void initiation, its growth, to line failure. The simulation has predicted accurately the lifetime as well as the failure site of the metal line. In the verification, however, the metal lines treated had the same grain size, that is, the same microstructure. In this article, the prediction method for the electromigration failure of polycrystalline lines was verified in more detail, by comparing the prediction results of lifetime and failure site with the results of experiments using not only various shaped lines but also lines whose microstructures were different. © 2000 American Institute of Physics. [S0021-8979(00)04406-6]

## I. INTRODUCTION

Electromigration is one of the key reasons of metal line failure in packaged silicon integrated circuit. It is essential in the study of reliability on integrated circuit to predict the lifetime of the metal line.

In order to predict the lifetime, the Black's equation<sup>1</sup> is generally used in extrapolating time to failure in the acceleration test to that under operating condition. The extrapolation by the Black's equation, however, is not able to universally predict the lifetime. The prediction result is changed by the choice of condition in the acceleration test,<sup>2</sup> and the acceleration tests to get the constant depending on line shape have to be performed for every line shapes even if the film characteristic is the same.

The lifetime of the metal line is closely associated with the formation of voids. The formation of voids and hillocks, that is, electromigration damage results from the divergence of atomic flux due to electromigration. Sasagawa *et al.*<sup>3</sup> have developed a formulation of the atomic flux divergence,  $AFD_{gen}$ , by considering all factors on electromigration damage, that is, current density, temperature, their gradients, microstructure of line and film characteristics, and they have identified  $AFD_{gen}$  as a parameter governing electromigration damage from the agreement of the void formation calculated by using  $AFD_{gen}$  with experiment. Recently, they also proposed a method to predict electromigration failure of polycrystalline line by using  $AFD_{gen}$ .<sup>4</sup> Lifetime and failure site in the metal line were predicted by a numerical simulation of

the processes of void initiation, its growth to line failure using  $AFD_{gen}$ , where the changes in the distributions of current density and temperature with void growth were taken into account. In that study, the prediction method was verified experimentally using various line shapes under various operating conditions. The current density and temperature distributions, which are effective factors on electromigration damage, are changed by the line shape and operating condition. Though mean-time-to-failure and failure location were changed by the line shape and operating condition, the lifetime and failure site were able to be predicted accurately with this method.

The experimental verification, however, treated the test lines which were the same in grain size, that is, microstructure. Namely, the method was not verified taking notice of the microstructure of line. The microstructure is not only one of the effective factors on electromigration damage but also closely related to the morphology of void growth since the voids grow selectively along grain boundary in polycrystalline line. Therefore, it is important for verification of the prediction method's validity to clarify the effect of not only line shape and operating condition but also the microstructure on the results predicted based on the simulation of the growing process of a void. In the present article, the prediction method for the polycrystalline line failure using the governing parameter of electromigration damage,  $AFD_{gen}$ , is verified in more detail by comparing the prediction results of lifetime and failure location with the experimental results using not only various shaped lines but also lines which have different microstructures.

<sup>a)</sup>Electronic mail: sasagawa@cc.hirosaki-u.ac.jp

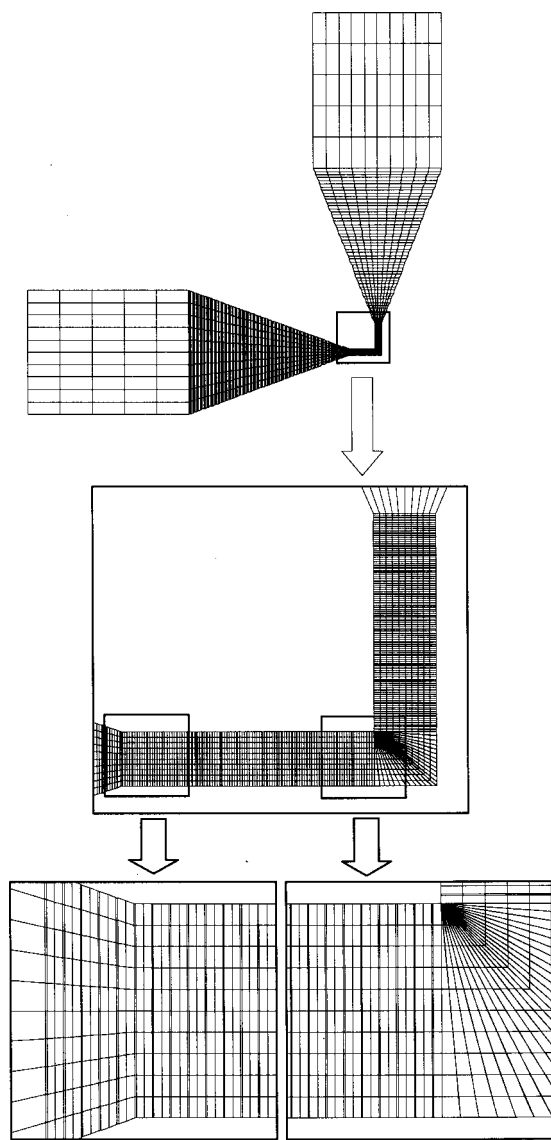


FIG. 1. Example of the finite element mesh and its enlargement of the testing part of specimen. The exclusive elements to constitute the slit-like void are allocated in the mesh generation as illustrated by very slim rectangle.

## II. PREDICTION METHOD

### A. Calculation method of $AFD_{gen}$

The governing parameter of electromigration damage,  $AFD_{gen}$ , has been proposed by Sasagawa *et al.*<sup>3</sup> for both cases of polycrystalline line and bamboo line. Here, the summary of the calculation method of  $AFD_{gen}$  for polycrystalline line is shown. The parameter  $AFD_{gen}$  has been formulated as follows;

$$AFG_{gen} = \frac{1}{4\pi} \int_0^{2\pi} (AFD_{gb\theta} + |AFD_{gb\theta}|) d\theta, \quad (1)$$

where

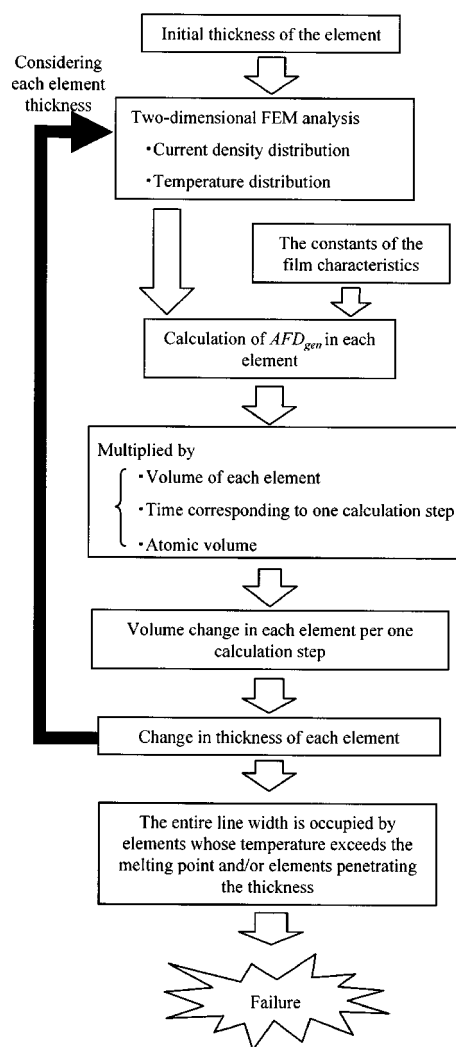


FIG. 2. Computation procedure for the numerical simulation of the processes of line failure. The thickness of only the slit-like element is changed by this procedure.

$$AFD_{gb\theta} = C_{gb}\rho \frac{4}{\sqrt{3}b^2} \frac{1}{T} \exp\left(-\frac{Q_{gb}}{kT}\right) \times \left\{ \sqrt{3}\Delta\varphi(j_x \cos\theta + j_y \sin\theta) - \frac{b}{2}\Delta\varphi \right. \\ \times \left[ \left(\frac{\partial j_x}{\partial x} - \frac{\partial j_y}{\partial y}\right) \cos 2\theta + \left(\frac{\partial j_x}{\partial y} + \frac{\partial j_y}{\partial x}\right) \sin 2\theta \right] \\ \left. + \frac{\sqrt{3}b}{4T} \left(\frac{Q_{gb}}{kT} - 1\right) \left(\frac{\partial T}{\partial x} j_x + \frac{\partial T}{\partial y} j_y\right) \right\}. \quad (2)$$

The quantity  $C_{gb}$  is a constant related to the atomic density, the diffusion coefficient, effective charge, and effective width of grain boundary, and takes negative value,  $T$  is the absolute temperature, the temperature-dependent resistivity  $\rho$  is expressed as  $\rho = \rho_0[1 + \alpha(T - T_s)]$ , where  $\rho_0$  is the resistivity and  $\alpha$  is the temperature coefficient at substrate temperature,  $T_s$ ,  $b$  is the average grain size,  $Q_{gb}$  is the activation energy for dominant grain boundary diffusion,  $k$  is the Boltzmann's constant, and  $\Delta\varphi$  is a constant associated with the

	A [ $\mu\text{m}$ ]	B [ $\mu\text{m}$ ]	Grain Size [ $\mu\text{m}$ ]	Effective Width of Slit [ $\mu\text{m}$ ]	Input Current Density [ $\text{MA}/\text{cm}^2$ ]	$T_s$ [K]
Sample 1	83	19.8	0.8	0.056	7.3	373
Sample 2	83	19.8	0.5	0.040	7.3	373
Sample 3	42	9.8	0.8	0.056	9.0	358
Sample 4	42	9.8	0.5	0.040	9.0	358

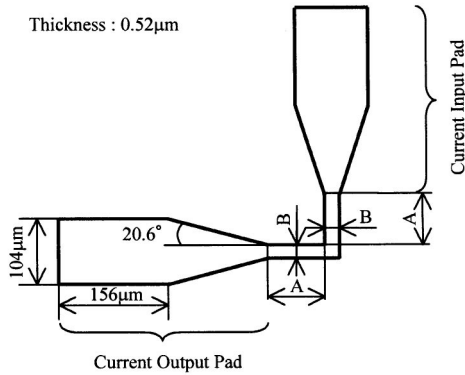


FIG. 3. Four aluminum lines used to predict the lifetime and failure site. Testing conditions for the four lines, Samples 1, 2, 3, and 4, are also shown in this figure.

relative angle of the grain boundaries. These constants represent film characteristics and are determined by acceleration test using straight shaped line.<sup>4</sup> The formulas of Eqs. (1) and (2) are applicable to not only straight shaped line, which results in uniform current density and one-dimensional temperature distribution, but also complicated shaped line such as an angled line, which results in two-dimensional distributions of current density and temperature. The quantities  $j_x$  and  $j_y$  are the components of current density vector  $\mathbf{j}$  in Cartesian coordinates  $x$  and  $y$ . The value of  $\text{AFD}_{\text{gen}}$  gives the change in number of atoms per unit volume and unit time.

The distributions of the current density and temperature given to the formulas are obtained by numerical analysis.

TABLE I. Constants used in the simulation.

	Sample 1	Sample 2	Sample 3	Sample 4
$\rho_0$	$4.85 \times 10^{-2}$	$4.55 \times 10^{-2}$	$4.61 \times 10^{-2}$	$4.39 \times 10^{-2}$
( $\Omega \mu\text{m}$ )	(at 373 K)	(at 373 K)	(at 358 K)	(at 358 K)
$\alpha$	0.00320	0.00320	0.00336	0.00336
(/K)	(at 373 K)	(at 373 K)	(at 358 K)	(at 358 K)
$b$	0.8	0.5	0.8	0.5
( $\mu\text{m}$ )				
$Q_{\text{gb}}$	0.6254	0.5532	0.6254	0.5532
(eV)				
$\Delta\phi$	-1.35	-1.33	-1.35	-1.33
(deg)				
$C_{\text{gb}}$	$1.99 \times 10^{18}$	$2.27 \times 10^{17}$	$1.99 \times 10^{18}$	$2.27 \times 10^{17}$
(KC/Js)				
$\lambda$	$2.33 \times 10^{-4}$	$2.33 \times 10^{-4}$	$2.33 \times 10^{-4}$	$2.33 \times 10^{-4}$
[W/( $\mu\text{m K}$ )] <sup>a</sup>				
$H$	$1.7 \times 10^{-6}$	$1.6 \times 10^{-6}$	$2.2 \times 10^{-6}$	$2.2 \times 10^{-6}$
[ $\bar{W}/(\mu\text{m}^2 \text{K})$ ]				
Effective width of slit ( $\mu\text{m}$ )	0.056	0.040	0.056	0.040

<sup>a</sup>Reference 6.

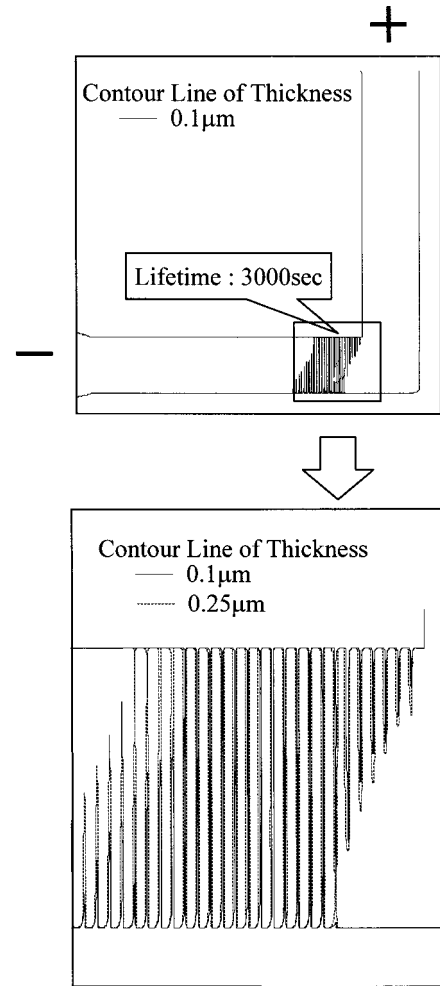


FIG. 4. Prediction results of the lifetime and failure site in the case of Sample 1. The metal line failure was predicted to occur with 3000 s in lifetime and at cathode side of corner in failure site.

The fundamental equations in the analysis are expressed as follows.

Governing equation concerning electrical potential  $\phi_e$ :

$$\nabla^2 \phi_e = 0. \quad (3)$$

Ohm's law:

$$i = -\frac{1}{\rho_0} \text{grad } \phi_e. \quad (4)$$

Equation of steady-state heat conduction:<sup>5</sup>

$$\lambda \nabla^2 T + \rho_0 \mathbf{j} \cdot \mathbf{j} + (\rho_0 \alpha \mathbf{j} \cdot \mathbf{j} - H)(T - T_s) = 0, \quad (5)$$

where the electric resistivity in the electrical problem is assumed to be constant with sufficient approximation,  $\lambda$  is the thermal conductivity,  $H$  is the constant concerning the heat flow from the line to the substrate, and  $\nabla^2 = \partial^2/\partial x^2 + \partial^2/\partial y^2$ .

## B. Numerical simulation using $\text{AFD}_{\text{gen}}$

Lifetime and failure site in the polycrystalline line are predicted by means of numerical simulation of the processes of a void initiation, its growth to line failure using  $\text{AFD}_{\text{gen}}$

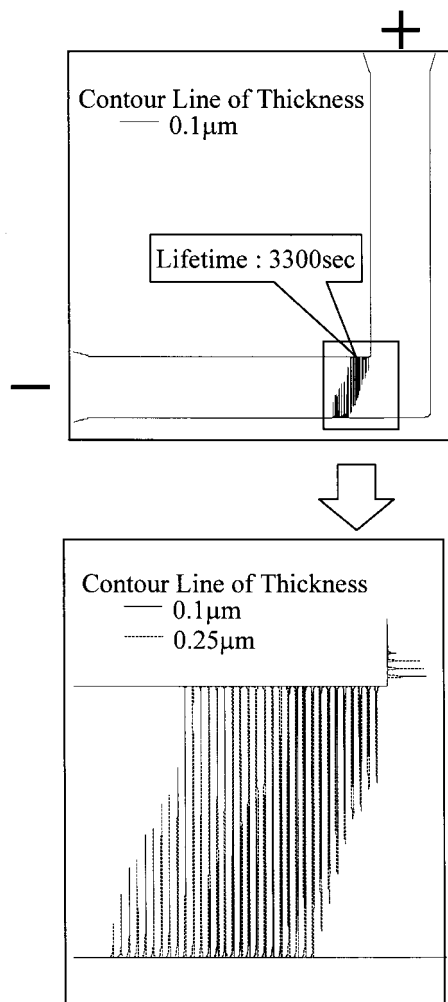


FIG. 5. Prediction results of the lifetime and failure site in the case of Sample 2. The failure was predicted to happen with 3300 s in lifetime and at the cathode side of corner in failure site.

for polycrystalline line, where the changes in distributions of current density and temperature with void growth are taken into account on the calculation of  $AFD_{gen}$ .

In the numerical simulation, the metal line is divided into elements as shown in Fig. 1 and the failure process is simulated by decreasing the element thickness based on  $AFD_{gen}$ . Considering the morphology of void growth in polycrystalline line, that is, voids grow selectively along grain boundary, resulting in slit-like voids extending toward the linewidth and linking each other, the element thickness is decreased at only very slim elements which are allocated based on measurements of average grain size and effective width of slit-like void in objective line.<sup>4</sup> The pitch and width of the very slim elements equal the average grain size and the effective width of slit-like void.

Computation procedure is shown in Fig. 2. At first, the distributions of current density and temperature in the metal line are obtained by a two-dimensional FEM analysis. The divergence  $AFD_{gen}$  in each element is calculated by using these distributions and the constants of the film characteristics which are determined in advance from the acceleration test.<sup>4</sup> The volume decreasing in each element per one calculation step in the simulation is given by multiplying the vol-

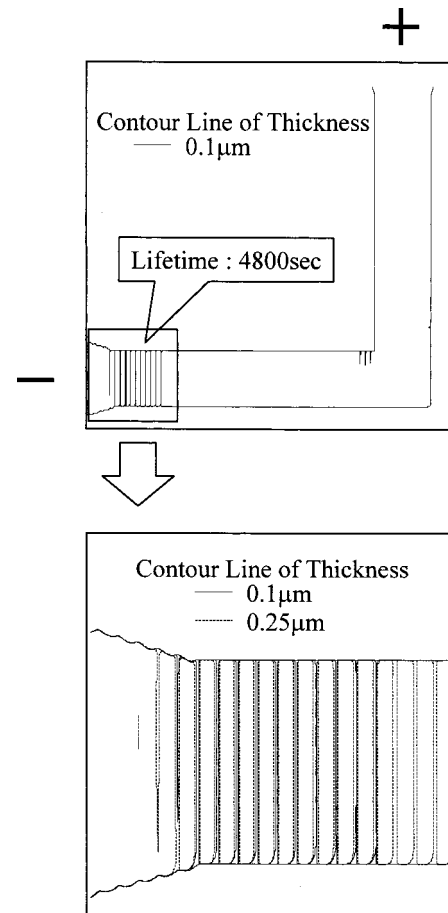


FIG. 6. Prediction results of the lifetime and failure site in the case of Sample 3. The predicted lifetime was 4800 s and failure site was cathode end.

ume of each element, the time corresponding to one calculation step and the atomic volume to the value of  $AFD_{gen}$ , where one calculation step is assigned to realistic time. The thickness of only the element for the slit-like void is decreased using the decrement of element volume calculated in the element and the neighboring elements, but the neighboring elements do not change in the thickness. In the element whose thickness is decreased, the void whose depth corresponds to the decrement in the thickness of the element is regarded as be formed. The FEM analysis of current density and temperature in the metal line is carried out again considering every element thickness. The calculation shown in Fig. 2 is carried out repeatedly.

Considering the change in thickness of the exclusive elements for the slit, the calculation process of the numerical simulation for the lifetime prediction is carried out repeatedly until metal line fails which is defined as the state that the entire linewidth is occupied by elements whose temperature exceeds the melting point and/or elements penetrating the thickness. Here, the element thickness smaller than an infinitesimal threshold value is considered to be penetrating. The threshold value is found so that the predicted lifetime is enough converged in numerical simulation. The threshold value used is  $3 \times 10^{-3}$  times the initial thickness. Thus, the



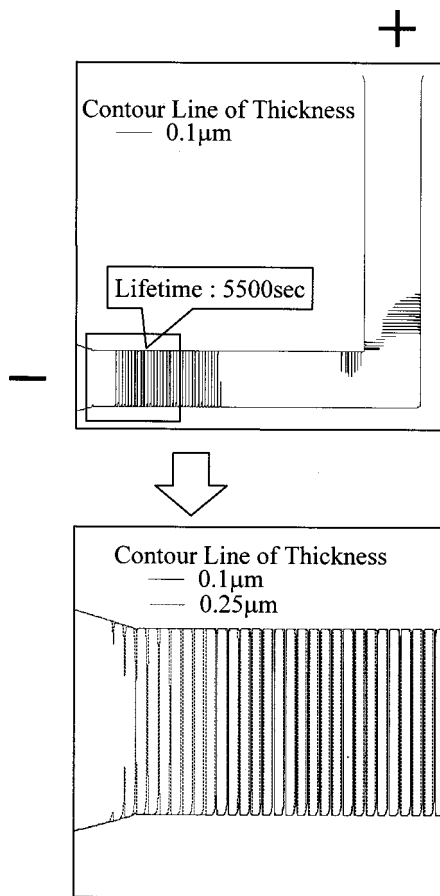


FIG. 7. Prediction results of the lifetime and failure site in the case of Sample 4. It was predicted that lifetime was 5500 s and failure site was cathode end.

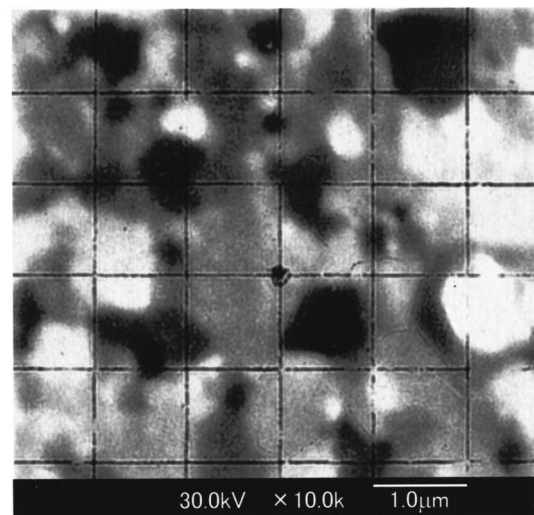
numerical simulation predicts the lifetime and the failure site of the metal line under operating condition.

### III. VERIFICATION OF THE PREDICTION METHOD

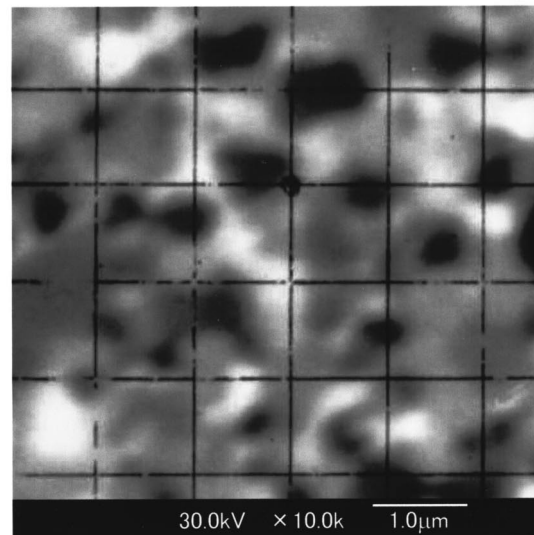
#### A. Prediction

To predict the lifetime and failure site, the aluminum polycrystalline lines shown in Fig. 3 were used. It was noted that the angled metal line results in two-dimensional distributions of current density and temperature. Four kinds of lines, which had two kinds of average grain sizes for each two kinds of line shapes, were supposed. Let us call the four lines Samples 1, 2, 3, and 4 as shown in Fig. 3. High current density and temperature, relative to the general operating condition, were chosen as the testing conditions to reduce the time required for experiment of the verification. The film characteristic constants to calculate  $AFD_{gen}$  and the effective width of slit-like void were obtained by the acceleration test using straight shaped lines<sup>4</sup> as listed in Table I. Average grain size was measured by using a focused ion beam (FIB) equipment. By performing the numerical simulation, electromigration failure was predicted for each sample.

The prediction results are shown in Fig. 4 to Fig. 7 for each sample. In the case of Sample 1, the metal line failure was predicted to occur with 3000 s in lifetime and at cathode side of corner in failure site. And the failure was predicted



(a)



(b)

FIG. 8. Examples of FIB observation of aluminum grains: (a) the average grain size is approximately  $0.8 \mu\text{m}$  (Samples 1 and 3), and (b) the average grain size is approximately  $0.5 \mu\text{m}$  (Samples 2 and 4).

for Sample 2 to happen with 3300 s in lifetime and at the cathode side of corner in failure site. For Sample 3, predicted lifetime was 4800 s and failure site was cathode end. And in the case of Sample 4, it was predicted that lifetime was 5500 s and failure site was cathode end.

#### B. Experiment

In order to verify the results of the prediction, experiment was performed concerning the same line dimension and condition as those in the simulation. Ten specimens were used for each sample. Aluminum film was deposited by vacuum evaporation on silicon substrate which was covered with silicon oxide. The specimens were patterned by etching after annealing. By changing the time of annealing, 30 and 60 min, two average grain sizes shown in Fig. 8 were provided for each line shape. The experiment was performed

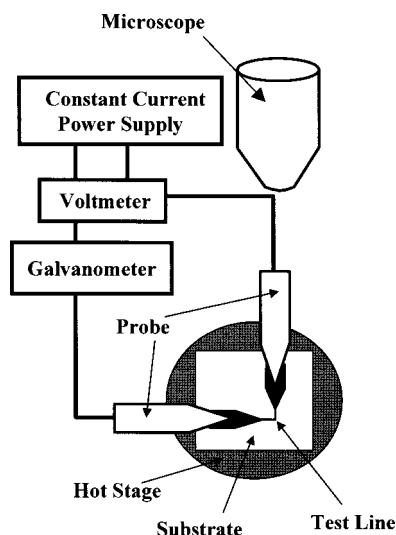


FIG. 9. Experimental setup. Test line is kept at a fixed temperature on the hot stage and subjected to dc current flow using the constant current power supply through the galvanometer and probes.

using an experimental setup shown in Fig. 9 until the metal line becomes open, and after that the specimen was observed by scanning electron microscope (SEM).

Figures 10–13 show the experimental results with fre-

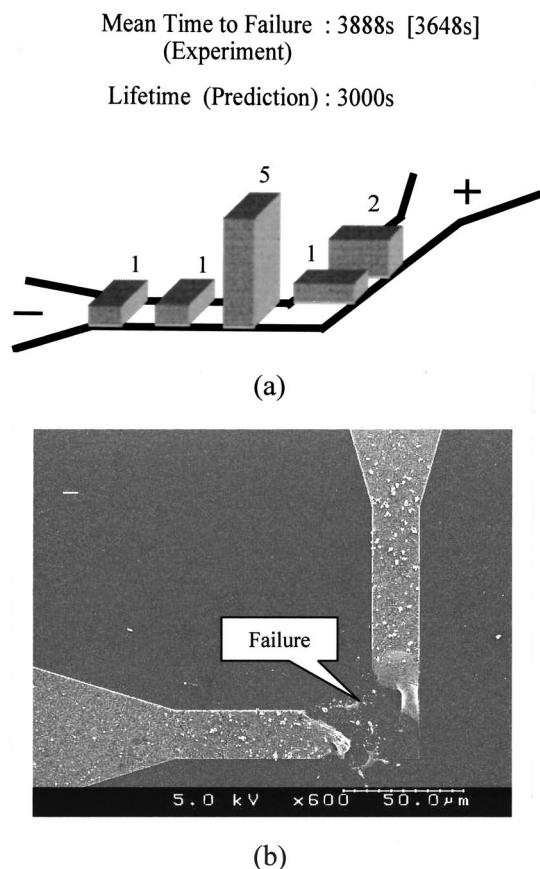


FIG. 10. Experimental results of Sample 1: (a) frequency distribution of the failure site with mean-time-to-failure, where mean-time-to-failure (experiment) without square brackets was obtained from ten specimens and that in brackets was obtained from five specimens which failed at the cathode side of the corner, and (b) an example of SEM observation of failure site.

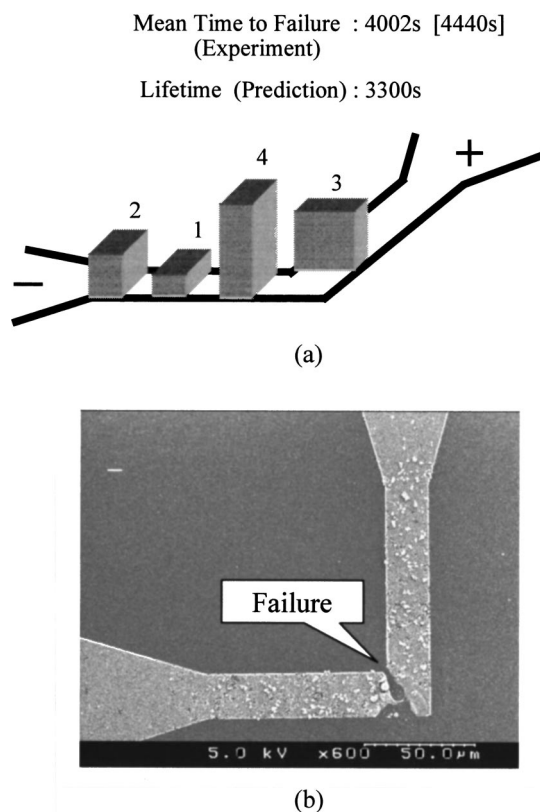


FIG. 11. Experimental results of Sample 2: (a) frequency distribution of the failure site with mean-time-to-failure, where mean-time-to-failure (experiment) without square brackets was obtained from ten specimens and that in brackets was obtained from four specimens which failed at the cathode side of the corner, and (b) an example of SEM observation of failure site.

quency distribution of the failure site in the line and the mean-time-to-failure. In the case of Sample 1, the mean-time-to-failure obtained from all the ten specimens was 3888 s and the most frequent failure site was cathode side of corner. The mean-time-to-failure from five specimens which opened at the predicted failure site, that is, cathode side of corner was 3648 s. The mean-time-to-failure obtained from all the ten specimens was 4002 s and the cathode side of corner was the most frequent site for Sample 2. The mean-time-to-failure from four specimens which opened at the predicted failure site, that is, the cathode side of the corner was 4440 s. For Sample 3, the mean-time-to-failure obtained from all the ten specimens was 4386 s and the cathode end of the line was the most frequent site. The mean-time-to-failure from six specimens which opened at the predicted failure site, that is, the cathode end of the line was 4980 s. And for Sample 4, the mean-time-to-failure obtained from all the ten specimens was 5898 s and the cathode end of the line was the most frequent site. The mean-time-to-failure from six specimens which opened at the predicted failure site, that is, the cathode end of the line was 5480 s. The mean-time-to-failure from specimens which opened at the predicted failure site was close to that from ten specimens in all samples.

The failure site somewhat spread in the experiment, but the most frequent site was predicted in all samples. In both prediction and experiment, the lifetime of the line having small grains was longer than that of the line having large

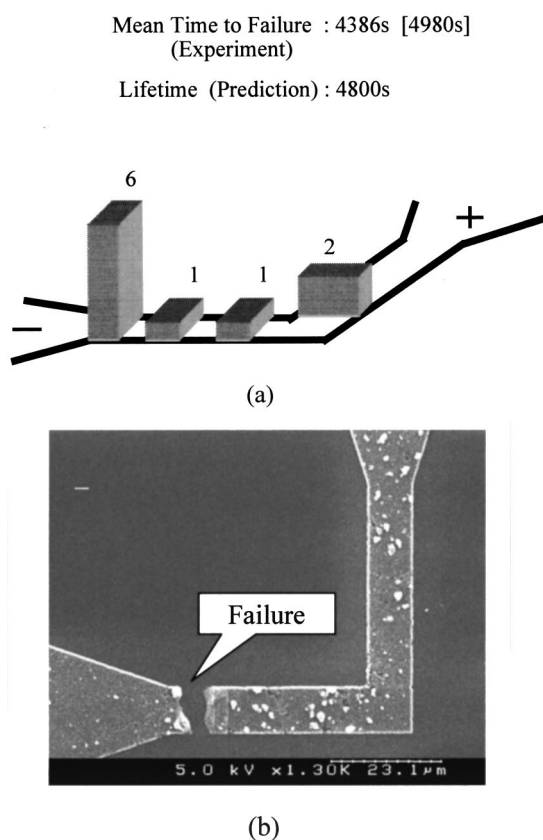


FIG. 12. Experimental results of Sample 3: (a) frequency distribution of the failure site with mean-time-to-failure, where mean-time-to-failure (experiment) without square brackets was obtained from ten specimens and that in brackets was obtained from six specimens which failed at the cathode end, and (b) an example of SEM observation of failure site.

grains, though it is generally known that the lifetime becomes longer with an increase in grain size. It is considered that this results from change in not only grain size but also film characteristics, for example, electric resistivity, by additional annealing. Anyway, the mean-time-to-failure and failure location were changed by line shape and operating condition, which affect on current density and temperature distributions, and by average grain size, that is, microstructure. Nevertheless, good agreement between the prediction and the experimental results was obtained in the lifetime and the failure site. From this it was shown that once the film characteristics were given, the lifetime and the failure site of the polycrystalline line which has any shape and any microstructure under arbitrary condition were able to be predicted by means of the numerical simulation using the governing parameter of electromigration damage,  $AFD_{gen}$ .

#### IV. CONCLUSIONS

The predicted lifetimes agreed well with the experimental results for various line shapes under various conditions even if the microstructure of the lines was different. And, about the failure site, although experimental results somewhat spread, the most frequent site coincided with the pre-

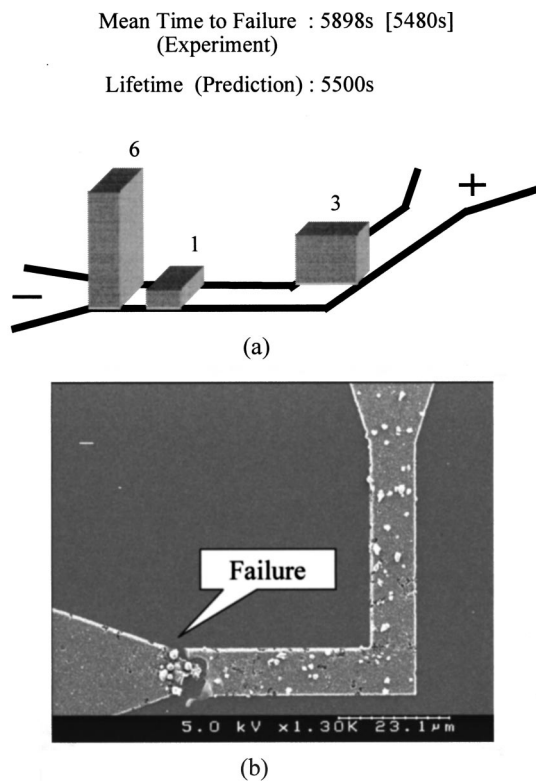


FIG. 13. Experimental results of Sample 4: (a) frequency distribution of the failure site with mean-time-to-failure, where mean-time-to-failure (experiment) without square brackets was obtained from ten specimens and that in brackets was obtained from six specimens which failed at the cathode end, and (b) an example of SEM observation of the failure site.

dicted failure site. Thus, the usefulness of the prediction method for polycrystalline line failure using the governing parameter of electromigration damage,  $AFD_{gen}$ , was verified in more detail.

#### ACKNOWLEDGMENTS

This work was partly supported by the Ministry of Education, Science, Sports and Culture under Grant-in-Aid for Encouragement of Young Scientists 10750058 and Grant-in-Aid for Scientific Research (B)(2) 10555024. A part of this work was performed in Venture Business Laboratory in Tohoku University.

<sup>1</sup>J. R. Black, Proc. IEEE **57**, 1587 (1969).

<sup>2</sup>J. W. McPherson, Proceedings of the IEEE International Reliability Physics Symposium, 1986, p. 12.

<sup>3</sup>K. Sasagawa, N. Nakamura, M. Saka, and H. Abé, Trans. ASME, J. Elect. Pack. **120**, 360 (1998).

<sup>4</sup>K. Sasagawa, K. Naito, M. Saka, and H. Abé, J. Appl. Phys. **86**, 6043 (1999).

<sup>5</sup>R. Kirchheim and U. Kaeber, J. Appl. Phys. **70**, 172 (1991).

<sup>6</sup>L. F. Mondolfo, Aluminum Alloys: Structure and Properties (Butterworths, London, 1976), p. 59.